Desalination and Water Treatment
www.deswater.com

doi: 10.5004/dwt.2021.26982

220 (2021) 380–391
April

Residence time distribution studies and modeling of rotating biological contactor reactor for decolorization of Congo red from synthetic dye wastewater

P. Vairavel[a], V. Ramachandra Murty[b,*]

[a]*Department of Chemical Engineering, Manipal Institute of Technology, Manipal Academy of Higher Education (MAHE), Manipal, Tel. +91 9036270978; email: pvairavel@gmail.com*
[b]*Department of Biotechnology, Manipal Institute of Technology, Manipal Academy of Higher Education (MAHE), Manipal, Tel. +91 9448529691; email: murty.vytla@manipal.edu (V. Ramachandra Murty)*

Received 24 July 2020; Accepted 21 December 2020

ABSTRACT

A continuous study in a rotating biological contactor (RBC) reactor was carried out using polyurethane foam (PU) surface-immobilized live fungal biomass of *Neurospora crassa* with wheat bran adsorbent/substrate for the removal of Congo red (CR) color from aqueous solutions. Residence time distribution studies were conducted at various flow rates of water (1–6.5 mL min^{-1}) using pulse input of tracer to explore the performance of mixing and type of flow behavior inside the reactor. It was found that the value of dispersion number at various flow rates of water such as 1, 3, and 6.5 mL min^{-1} was 4.36, 7.89, and 13.65, respectively, which indicates that the RBC reactor can be modeled as a mixed flow reactor. A model for a single stage RBC reactor for the decolorization of CR from synthetic dye wastewater has been developed using the principles of conservation of mass. Using the developed mathematical model and experimental data, the model parameters such as maximum specific growth rate of the attached active biomass (μ_{max}), Monod kinetic constant (K_s), rate constant for pseudo-second-order biosorption (K_2), and effluent dye concentration at equilibrium (S_e) were estimated. The system of non-linear first-order ordinary differential mass balance equation was solved by the fourth-order Runge–Kutta method and the model parameters were evaluated using the Solver tool in Excel. The predicted and experimental values of effluent dye concentrations are then compared. The predicted values of effluent concentrations found from the theoretical model developed fitted well to the experimental data, suggests that the proposed model is valid for CR dye decolorization. The results reveal that the live fungal biomass of *N. crassa* with wheat bran is a suitable dual adsorbent for decolorization of CR from synthetic effluents using RBC reactor and it can be used effectively in wastewater treatment.

Keywords: Congo red dye; *Neurospora crassa*; Wheat bran; Residence time distribution; Dispersion number; Mathematical model

1. Introduction

Industrial wastewater is one of the important sources of pollution of the water environment. Synthetic dyes are extensively used in the textile dyeing, paper printing, plastic, leather cosmetics, rubber, and photography industries [1]. Among the various industrial sectors, textile industries are one of the most common and essential which generate a large volume of wastewater with varying physicochemical characteristics [2]. These colored effluents can be mixed with surface water streams and groundwater systems, contaminating sources of potable water [3]. The removal of toxic pollutants from the effluent before discharging into natural water bodies is extremely important from an environmental point of view. The synthetic dye CR is a water-soluble diazo anionic acidic dye prepared by

* Corresponding author.

coupling tetra-azotised benzidine with two molecules of naphthionic acid. Azo dyes are highly toxic, mutagenic, carcinogenic, and usually constitute health hazards [4]. Most of the azo dyes have been reported to be the main cause for bladder cancer in humans, splenic sarcomas, hepatocarcinomas, and chromosomal aberration in mammalian cells [5]. CR is considered as toxic due to its metabolism to benzidine, a human carcinogen and its exposure causes an allergic dermatitis, skin, eye, and gastrointestinal irritation [6]. It is investigated as a mutagen and reproductive effector. It may affect blood factors such as clotting, and induce somnolence and respiratory problems [7]. Even a low concentration of CR dye causes various harmful effects such as difficulties in breathing, diarrhea, nausea, vomiting, abdominal and chest pain, severe headache, etc. [8,9]. It has a strong affinity for cellulose fibers and thus is used in textile processing industries [10]. It is used as a laboratory aid for testing free hydrochloric acid in gastric contents, in the diagnosis of amyloidosis, as an indicator of pH, and also as a histological stain for amyloid [11,12].

Several methods including physical, chemical, and biological treatments have been developed to treat dye containing wastewater [13]. Among these techniques, adsorption is believed to be most promising because of its easy operation, low cost, and high performance without formation of harmful by-products (insensitivity to toxic pollutants) [14]. Effluents containing azo dyes from the textile industry are very difficult to treat using conventional treatment methods (excluding adsorption and biological treatment), because dyes are structurally complex and stable aromatic organic compounds [15]. The use of live cells for large scale process utilization has some problems such as low biomass growth rate, enzyme reutilization, and restriction of enzyme mobility [16]. To rectify these problems, the live cells can be immobilized on the surface of the bio-support materials by weak van der Waals forces. The proper realization of the live cells in a real effluent treatment system is based on the selection of a suitable reactor. Among the various reactor systems present for wastewater treatment, the aerobic rotating biological contactor (RBC) reactor is the most effective in treating complex substances present in the effluents [17]. In the RBC reactor, degrading microorganisms are grown by surface-immobilized live biomass onto the rotating discs of the reactor. Various studies on the removal of color from dye wastewater in a RBC reactor have been reported in the literature using several fungal species. This includes *Phanerochaete chrysosporium*, *Trametes versicolor*, *Dichomittus squalens*, and *Coriolus versicolor* [18]. Decolorization of selected toxic dye compounds with a few types of live fungal biomass and the use of agricultural by-product as a low-cost adsorbent of dye molecules has been studied [18–20]. The literature survey indicates that the study of color removal from dye effluents using live biomass with agricultural waste is limited. However, studies on the decolorization of CR dye from contaminated water in a RBC reactor using *Neurospora crassa* live biomass with wheat bran adsorbent/substrate is an area that has not been explored much. Experiments need to be performed to make use of fungus, grown in a simple, inexpensive medium with higher growth rates and maximum decolorization efficiency in the effluent. The conventional techniques are not available in the literature for the evaluation of the mixing performance of continuously operated systems [21]. To the best of our knowledge, there are no residence time distribution (RTD) studies in a RBC reactor available in literature evaluating the non-ideality of the system. In addition, there are no RBC reactor studies that have been reported for describing the ability of surface immobilized *N. crassa* live biomass with wheat bran adsorbent/substrate for the removal of CR dye from aqueous solutions. The combination of live biomass with wheat bran has the advantage of both being rapid and having a better decolorization efficiency in the removal of color from dye wastewater as compared to the individual substances [22]. Studies need to be conducted to make the use of *N. crassa* live biomass with wheat bran for the removal of color from CR dye wastewater in a RBC reactor. Therefore, an effort has been made to remove color from CR dye from wastewater using live biomass with wheat bran in a RBC reactor. *N. crassa* (the common pink bread mould) is a filamentous non-pathogenic ascomycete fungus that can be easily grown in a nutrient broth medium [23]. The fungal cell wall is composed of randomly disposed skeletal microfibrils of chitin, β-glucans, and protein containing a high percentage of the amides of aspartic and glutamic acid with several functional groups (amino, carboxyl, etc.), which are capable of binding toxic molecules in the effluent [24]. The outside diameter of the pore system is 40–70 Å embedded in the matrix of the wall [25]. Wheat bran is the outer shell of wheat grain, and an agricultural by-product of the wheat milling operation [13]. Wheat bran is an excellent source of hemicellulose and it is a good inducer of the cellulolytic enzyme system. It consists of cellulose (25%), hemicellulose (33%), starch (19%), crude protein (18%), and lipids (5%) [26]; furthermore, it is an economically viable and widely available natural material in India. Hence, RTD studies are performed to investigate the type of flow and non-ideality of the system, which has been used to develop a mathematical model. The combined biomass growth and biosorption kinetic model in the mass balance equation is applied to experimental data to evaluate the model parameters. With the advancement of computer simulations, a model using the resolution of the ordinary differential mass balance equation has been developed. The differential equation was solved using an appropriate numerical method and the model parameters were estimated using the software Excel Solver. Therefore, the present paper focuses on a model developed to describe the behavior of single stage RBC reactor for the removal of CR color from an aqueous solution using PU surface immobilized live fungal biomass of *N. crassa* with wheat bran adsorbent/substrate.

2. Materials and methods

2.1. Preparation of agricultural by-product wheat bran and N. crassa live biomass

Wheat bran is procured from M/s Ganesh Flourmill Industries, Kolkata, India. It is washed with distilled water to remove soluble impurities. The detailed procedure for preparation of wheat bran adsorbent/substrate and evaluation of optimized value of wheat bran dosage is given

in our previous study published elsewhere [22]. The fungus *N. crassa* (microbial type culture collection, MTCC 1852) used in this study was obtained from the Institute of Microbial Technology, Chandigarh, India, and was stored at 277 K. The detailed procedure for preparation of live fungal biomass is given elsewhere [22].

2.2. Chemicals required

An anionic dye, Congo red (dye content ≥35%, molecular formula = $C_{32}H_{22}N_6Na_2O_6S_2$, molecular weight = 696.66, and λ_{max} = 498 nm) supplied by Sigma Aldrich, India is used in the study. The dye is of analytical reagent grade, and of 99.8% purity. The analytical grade malt extract broth (MEB) and malt extract agar are obtained from Himedia, India. All other chemicals used are of analytical grade (Merck, India Limited).

2.3. Preparation of CR dye stock solution

The required amount of CR dye powder is dissolved in distilled water to prepare a 1,000 mg L^{-1} stock solution. This stock solution is further diluted with pH adjusted distilled water by adding 0.1 N HCl or 0.1 N NaOH to obtain the required concentration range. After dilution (adjusting the pH), the final pH of the dye solution is measured as 6 and further decolorization experiments are carried out at pH 6, because the red color remained stable in the pH range of 6–14. Batch studies results showed that maximum decolorization of CR is observed at pH 6. The detailed procedure for evaluation of optimized value of pH for CR dye removal is given elsewhere [22].

2.4. Analytical measurements

The pH of the dye solution is measured using a digital pH-meter (Systronics 335, India) and the unknown residual concentration of CR dye solution is measured at the wavelength (λ_{max}) of 498 nm using double-beam UV/visible spectrophotometer (Shimadzu UV-1800, Japan). The tracer concentration is measured using a conductivity meter (Systronics 335, India).

2.5. Experimental setup of the RBC reactor

A laboratory scale RBC reactor is constructed from polymethyl methacrylate sheet of 10 mm thickness. The RBC reactor was 74 cm in length, 21.4 cm in diameter, and 19 cm in height. The detailed experimental setup, design specifications of the RBC reactor, and the decolorization experimental procedure are reported in our previous study published elsewhere [20]. The % CR color removal is determined by Eq. (1) [20]:

$$\%\ \text{CR color removal} = \frac{\left(S_0 - S\right)\times 100}{S_0} \tag{1}$$

where S_0 and S (mg L^{-1}) are the influent and effluent substrate (CR dye) concentrations at initial time, t_0 and at time, t, respectively.

2.6. Tracer experiments in a RBC reactor

A unique technique for studying the performance of mixing, flow pattern and non-ideality in a reactor is the analysis of tracer-response profiles [27]. The RTD studies are performed by the stimulus-response technique using sodium chloride (NaCl) as a tracer (sodium chloride is an inorganic salt electrolyte and does not interfere with the solution) to verify the ideal behavior of the system [28]. Conductivity measurement is done at the reactor exit, with a probe inserted into a specially designed mixing cup of volume 100 mL. A 100 mL sample of 2.5 M NaCl solution is injected as a pulse input (injected rapidly) in the influent stream. Effluent samples are collected immediately after the injection and at regular time intervals, until no tracer is detected [29]. The operation is continued until the NaCl concentration at the outlet end reached its initial concentration in tracer-free tap water [30]. The tracer experiments are conducted at various flow rates of water ranging from 1 to 6.5 mL min^{-1}.

2.7. Theoretical investigation of RTD studies

The effluent concentration-time data from the stimulus response experiments are used to obtain the RTD parameters such as mean residence time, variance, and dispersion number. Residence-time distribution function also called as exit age distribution, $E(t)$ describes the distribution of times for the stream of fluid in the reactor. The RTD in the reactor is given by the $E(t)$ curve which describes the change in tracer concentration at the exit of the reactor. It is given by Eq. (2) [31]:

$$E\left(t\right) = \frac{C\left(t\right)}{\int_0^\alpha C\left(t\right)dt} \tag{2}$$

The mean residence time (t_m) is defined by the average transient time the material spends in the reactor and is calculated by the following expression [32]:

$$t_m = \frac{\int_0^\alpha t\ E\left(t\right)dt}{\int_0^\alpha E\left(t\right)dt} = \int_0^\alpha t\ E\left(t\right)dt \tag{3}$$

The variance (σ^2), that signifies spread of the tracer distribution is determined by Eq. (4) [31]:

$$\sigma^2 = \int_0^\alpha \left(t - t_m\right)^2 E\left(t\right)dt \tag{4}$$

The normalized RTD function, $E(\theta)$ can be defined as:

$$E(\theta) = t_m E\left(t\right) \tag{5}$$

$$\theta = \frac{t}{t_m} \tag{6}$$

where θ is the dimensionless parameter. When the function $E(\theta)$ is used, all perfectly mixed continuous stirred

tank reactors (CSTRs) have numerically the same RTD. If the simple function $E(t)$ is used, the numerical values of $E(t)$ can differ substantially for different CSTRs [31]. The tracer experiments are performed under closed vessel state and the vessel dispersion number (D_Z/UL) is evaluated using Eq. (7) [31,32]:

$$\frac{\sigma^2}{t_m^2} = 2\left(\frac{D_Z}{UL}\right) - 2\left(\frac{D_Z}{UL}\right)^2\left(1 - e^{-\left(\frac{UL}{D_Z}\right)}\right) \tag{7}$$

where D_Z is the axial dispersion coefficient for flowing fluid ($m^2\ s^{-1}$), U is the superficial velocity ($m\ s^{-1}$), and L is the length of the reactor (m). The dispersion number characterizes the extent of axial dispersion of tracer in the reactor [33].

2.8. Mathematical description of model development in a continuous RBC reactor

Assume that complete mixing in the liquid volume is achieved by the turbulence caused by the rotation of the disc. The performance of RBC reactor for the removal of color from CR dye wastewater using *N. crassa* live biomass with wheat bran adsorbent/substrate is analyzed by a mass balance with respect to substrate across the reactor yields [34,35]:

$$\frac{dM}{dt} = M_i - M_0 + R_G - R_C - R_{Ad} \tag{8}$$

where M is the mass of component "A" (CR dye solution) in the reactor (g); t is the effluent treatment time (h); M_i is the mass flow rate of "A" entering to the reactor ($g\ h^{-1}$); M_0 is the mass flow rate of "A" leaving from the reactor ($g\ h^{-1}$); R_G is the rate of mass generation of "A" by reaction ($g\ h^{-1}$); R_C is the rate of mass consumption of "A" by reaction ($g\ h^{-1}$); R_{Ad} is the rate of mass biosorption of "A" by wheat bran and live biomass in the reactor ($g\ h^{-1}$).

The substrate balance in the above system can be written as [34]:

Rate of accumulation = Rate of inflow – Rate of outflow + Rate of generation – Rate of consumption by attached growth – Rate of consumption by suspended growth – Rate of biosorption of CR by wheat bran and live biomass (9)

The rate of mass generation (R_G) of "A" is zero, because no new substrate is generated. The rate of substrate consumption by attached growth (R_{Ca}) and suspended growth (R_{Cs}) are expressed by Eqs. (10) and (11):

$$R_{Ca} = \frac{\mu_a A_w X_a}{Y_a} \tag{10}$$

$$R_{Cs} = \frac{\mu_s X_s V}{Y_s} \tag{11}$$

Substituting Eqs. (10) and (11) in Eq. (9), the mathematical expression for Eq. (8) can be written as [34,36]:

$$V\left(\frac{dS}{dt}\right) = FS_0 - FS - \frac{\mu_a A_w X_a}{Y_a} - \frac{\mu_s X_s V}{Y_s} - R_{Ad} \tag{12}$$

Batch experiments results shows that biosorption of CR by wheat bran and live biomass follows a pseudo-second-order kinetic model. Assuming that the overall rate of reaction is controlled by mass transfer, the kinetic rate Eq. (13) is given as [37]:

$$\frac{dq_t}{dt} = K_2\left(q_e - q_t\right)^2 \tag{13}$$

The mathematical representation of the parameters q_e and q_t are expressed by the following equations [38,39]:

$$q_e = \frac{\left(S_0 - S_e\right)V}{M_{LB-WB}} \tag{14}$$

$$q_t = \frac{\left(S_0 - S\right)V}{M_{LB-WB}} \tag{15}$$

where q_e and q_t are the equilibrium biosorption capacity and biosorption capacity at any time, t, respectively. Differentiating Eq. (15) with respect to time to get:

$$R_{Ad} = \frac{dq_t}{dt} = -\frac{dS}{dt}\frac{V}{M_{LB-WB}} \tag{16}$$

Substituting Eqs. (16) in (13) to get change in substrate concentration with time t based on biosorption:

$$-\frac{dS}{dt} = \frac{K_2 V}{M_{LB-WB}}\left(S - S_e\right)^2 \tag{17}$$

Assuming that the organism decay can be neglected because the decay rate is small compared to the growth rate. Substituting Eqs. (17) in (12) to get:

$$V\left(\frac{dS}{dt}\right) = FS_0 - FS - \frac{\mu_a A_w X_a}{Y_a} - \frac{\mu_s X_s V}{Y_s} - \frac{K_2 V^2}{M_{LB-WB}}\left(S - S_e\right)^2 \tag{18}$$

The consumption of substrate due to suspended growth can be neglected because the concentration of suspended biomass in this system is lower than that of the attached active biomass ($R_{Cs} <<< R_{Ca}$) [40].

where V is the volume of liquid in the reactor (L); dS/dt is the change in substrate concentration with time ($mg\ L^{-1}\ h^{-1}$); F is the flow rate of dye solution ($mL\ min^{-1}$); S_0 is the influent substrate (dye) concentration ($mg\ L^{-1}$); S is the effluent substrate (dye) concentration ($mg\ L^{-1}$); S_e is the effluent substrate (dye) concentration at equilibrium ($mg\ L^{-1}$); μ_a is the specific growth rate of the attached biomass (h^{-1}); Y_a is the apparent yield coefficient of the attached biomass (mg biomass attached per mg substrate consumed); A_w is the total surface area of the bio-disc (m^2); X_a is the mass of attached active biomass per unit area of bio-disc ($mg\ m^{-2}$); μ_s is the specific growth rate of the suspended biomass (h^{-1}); Y_s is the apparent yield coefficient of the suspended biomass (mg biomass produced per mg

substrate consumed); X_s is the concentration of suspended biomass (mg L^{-1}); K_2 is the equilibrium rate constant of pseudo-second-order biosorption (g mg^{-1} h^{-1}); M_{LB-WB} is the mass of attached active live fungal biomass and wheat bran (g) existing in the reactor system before treatment of dye wastewater at time $t = 0$.

Net amount of attached biomass per unit area of bio-disc (X_a) is the difference between total amount of attached biomass per unit area of bio-disc in dye medium (X_d) and MEB medium (X_n):

$$X_a = X_d - X_n \tag{19}$$

In the simplified form, Eq. (18) can be written as:

$$\left(\frac{dS}{dt}\right) = \frac{F}{V}\left(S_0 - S\right) - \frac{\mu_a A_w X_a}{Y_a V} - \frac{K_2 V}{M_{LB-WB}}\left(S - S_e\right)^2 \tag{20}$$

The group of parameters $X_a A_w/V$ in Eq. (20) are expressed as X_f:

$$X_f = \frac{X_a A_w}{V} \tag{21}$$

Therefore:

$$\left(\frac{dS}{dt}\right) = \frac{F}{V}\left(S_0 - S\right) - \frac{\mu_a X_f}{Y_a} - \frac{K_2 V}{M_{LB-WB}}\left(S - S_e\right)^2 \tag{22}$$

The yield coefficient of attached active biomass can be written as [41]:

$$Y_a = \frac{X_f - X_0}{S_0 - S} \tag{23}$$

where X_f and X_0 are the concentrations of attached active biomass in dye and MEB medium (mg L^{-1}), respectively. Next, Eq. (23) is rearranged as:

$$X_f = \left(S_0 - S\right)Y_a + X_0 \tag{24}$$

A Monod model (Eq. (25)) is applied to estimate cell growth rate. It is related to growth rate and to the limiting substrate concentration. The specific growth rate of attached active biomass is given by the expression [42]:

$$\mu_a = \mu_{max}\left(\frac{S}{K_s + S}\right) \tag{25}$$

where μ_{max} is the maximum growth rate of attached active biomass (h^{-1}) and K_s is the Monod saturation constant for the rate-limiting substrate (mg L^{-1}). Substituting Eqs. (24) and (25) in Eq. (22), the substrate mass balance equation (Eq. (26)) can be written as follows:

$$\left(\frac{dS}{dt}\right) = \frac{F}{V}\left(S_0 - S\right) - \mu_{max}\left(\frac{S}{K_S + S}\right)\left[\frac{\left(S_0 - S\right)Y_a + X_0}{Y_a}\right] - \frac{K_2 V}{M_{LB-WB}}\left(S - S_e\right)^2 \tag{26}$$

Eq. (26) is a non-linear first-order ordinary differential equation (ODE). The numerical solution of ODE can be solved by the fourth-order Runge–Kutta method and the model parameters such as μ_{max}, K_s, K_2, and S_e were estimated by the software Excel Solver. The sum of square error (SSE) was estimated by Eq. (27) [43]:

$$\text{Sum of square error, SSE} = \left[\frac{\left(S_{expt} - S_{Pred}\right)^2}{\left(S_{expt}\right)^2}\right] \tag{27}$$

where S_{expt} and S_{pred} are the experimental and predicted values of effluent substrate concentration at time t, respectively.

3. Results and discussion

3.1. Analysis of RTD studies in the RBC reactor

The RTD data obtained at various flow rates of water are reported in Table 1. It shows that the mean residence time (t_m) is slightly higher than actual space time (τ) at a flow rate of 1 and 3 mL min^{-1}. It indicates that most of the tracer leaves the system and a small amount of tracer may remain stuck inside the reactor. There are a small number of hydraulic dead spaces and stagnant eddies that may exist in the reactor system. At a flow rate of 6.5 mL min^{-1}, the mean residence time is slightly lower than actual space time. It signifies that a very small degree of channeling and bypassing (no short-circuiting of fluid) may occur in the reactor system. The above result indicates that the RBC reactor system was working properly and efficiently (no accumulation of tracer compound). The E-curves obtained at various flow rates of water are shown in Fig. 1 (Figs. S1–S3). The normalized RTD function, $E(\theta)$ at various flow rates are shown in Fig. 2. Figs. 1 and 2 show that the distribution curve was wider and a long tail was obtained at various flow rates of water, which represents that, a significant degree of dispersion may be taking place in the reactor. Dispersion number was calculated by using the Solver tool in Microsoft Excel. A dispersion number of zero represents perfect plug flow (no spreading of tracer) and a value at infinity represents completely mixed flow [31,44]. Large dispersion number signifies the rapid spreading of the tracer curve, while smaller value represents slow spreading [45]. The value of dispersion number gradually increased from 4.36 to 13.65 with an increase in flow rate of water from 1 to 6.5 mL min^{-1}. This may be due to higher degree of dispersion taking place when hydraulic retention time was decreased significantly. A similar observation has been reported elsewhere [28]. The dispersion number value of 0.2 represents plug flow with large dispersion (good mixing) and a dispersion number of 0.02 represents plug flow with medium dispersion [46]. The dispersion number in this present study was greater than 4 at various flow rates of water illustrates that the RBC reactor can be modeled as a mixed flow reactor (concentration of the tracer spreads in the effluent may be uniform throughout the reactor). The value of the dispersion number quantitatively signifies the extent of non-ideality.

Table 1
RTD data obtained at various flow rates of water in a RBC reactor

Flow rate of water (mL min^{-1})	Space time, τ (d)	Mean residence time, t_m (d)	Variance, σ^2 (d^2)	Dispersion number (D_z/UL)
1	8.333	8.446	66.18	4.36
3	2.777	2.870	7.90	7.89
6.5	1.282	1.222	1.46	13.65

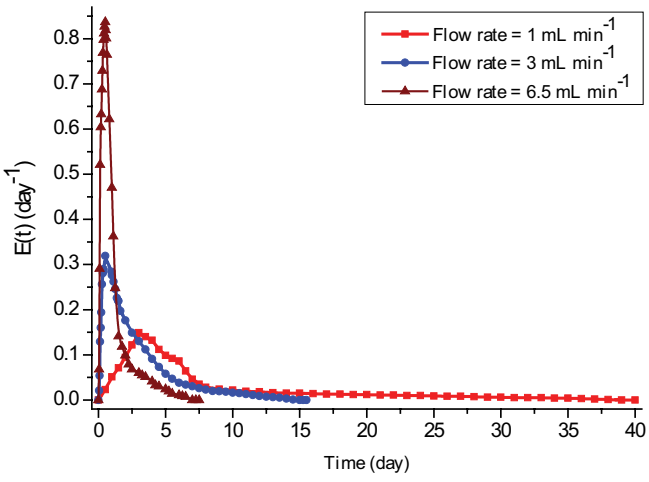

Fig. 1. Comparison of exit-age distribution function at various flow rates of water in the RBC reactor. (Volume of liquid in the reactor: 12 L; air flow rate: 1.5 L min^{-1}; number of discs: 20; disc rotation speed: 16 rpm; disc submergence in liquid medium: 40%; temperature: 303 K).

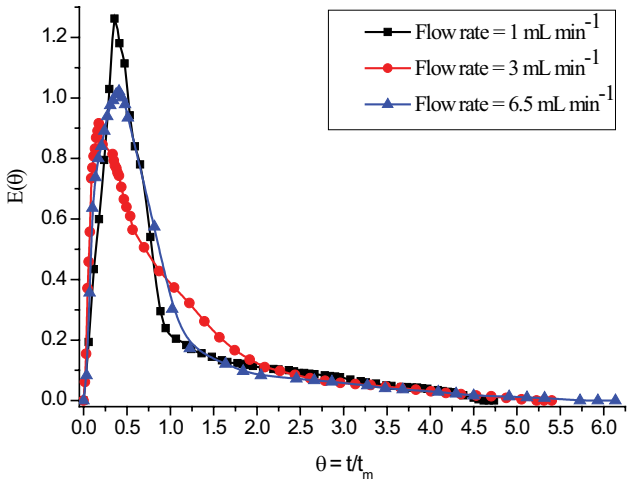

Fig. 2. Comparison of normalized distribution function at various flow rates of water in the RBC reactor. (Volume of liquid in the reactor: 12 L; air flow rate: 1.5 L min^{-1}; number of discs: 20; disc rotation speed: 16 rpm; disc submergence in liquid medium: 40%; temperature: 303 K).

3.2. Evaluation of model parameters at various operating conditions for CR dye decolorization in RBC reactor

A continuous study in a laboratory scale RBC reactor was carried out using PU surface immobilized live fungal biomass of *N. crassa* with wheat bran for the removal of color from synthetic CR dye wastewater at ambient temperature. The effect of fundamental parameters such as initial pH, initial dye concentration, wheat bran dosage, live biomass dosage, wheat bran particle size, and agitation speed on CR dye decolorization were studied and optimized using central composite design (CCD) to attain the maximum decolorization efficiency; this is given in our previous paper published elsewhere [22]. The effect of various process parameters such as number of discs, disc rotation speed, % disc submergence in liquid medium, flow rate of dye solution, air flow rate, wheat bran dosage, and inlet dyestuff concentration on CR dye decolorization were studied and this is given in our previous paper published elsewhere [20]. The decolorization of CR may be due to both biosorption and enzymatic decolorization process. It also infers that the first 2 d (48 h) biosorption is active, followed by the enzymatic decolorization process for the rest of the days [20]. The agricultural by-product wheat bran acts as an adsorbent and it also may act as a substrate for the growth of fungus which improves the decolorization efficiency. RTD data revealed that the concentration of liquid leaving from the reactor was uniform and complete mixing was attained due to the high rotational speed of the discs. Combined Monod and pseudo-second-order kinetic model in mass balance equation were applied to experimental data and the results of model parameters obtained at various operating conditions are shown in Table 2. It shows that the value of μ_{max} for the decolorization of CR at various operating conditions were in the range between 1.82×10^{-4} to 6.34×10^{-4} h^{-1}. The value of Monod constant, K_s at various operating conditions were in the range between 17 and 48 mg L^{-1}. The rate constant, K_2 decreased from 0.0154 to 0.0072 g mg^{-1} h^{-1} and the biosorption capacity at equilibrium, q_e increased from 2.656 to 13.649 mg g^{-1} with an increase in dye concentration from 50 to 500 mg L^{-1}. The decrease in the value of K_2 is may be due to decreased competition at the active sites on the *N. crassa* live biomass and wheat bran dual adsorbent surface at lower concentration and increased competition for the binding sites at higher concentrations [38]. The increase in the value of q_e is because of increase in concentration difference among the dye concentration in the solution and the surface of the dual adsorbent. This concentration gradient acts as a driving force for the diffusion of dye molecules from bulk solution to the dual adsorbent surface [39]. The results of biosorption at various flow rates of dye solution which are explained here are shown in Table 2. It shows that the biosorption of CR is dependent mainly on the flow rate. From Table 2, the equilibrium biosorption

Table 2
Combined Monod and pseudo-second-order kinetic model parameters at various operating conditions for CR dye decolorization in RBC reactor

Various operating parameters							Model parameters					
N_D	N (rpm)	D_{SL} (%)	Q_{air} (L min^{-1})	F (mL min^{-1})	M_{WB} (g L^{-1})	S_0 (mg L^{-1})	μ_{max} (h^{-1})	K_s (mg L^{-1})	K_2 (g mg^{-1} h^{-1})	$S_{e,expt}$ (mg L^{-1})	$S_{e,pred}$ (mg L^{-1})	q_e (mg g^{-1})
8	16	40	1.5	1	12.5	200	6.346×10^{-4}	41.334	0.0058	82.849	79.568	8.288
14	16	40	1.5	1	12.5	200	3.568×10^{-4}	25.459	0.0080	67.384	66.386	8.413
20	16	40	1.5	1	12.5	200	3.224×10^{-4}	33.831	0.0082	42.655	42.115	8.924
20	4	40	1.5	1	12.5	200	4.536×10^{-4}	25.036	0.0044	80.000	77.889	7.499
20	8	40	1.5	1	12.5	200	3.762×10^{-4}	30.355	0.0082	55.466	54.065	8.394
20	16	30	1.5	1	12.5	200	4.611×10^{-4}	35.537	0.0108	53.000	51.432	6.702
20	16	35	1.5	1	12.5	200	4.199×10^{-4}	28.056	0.0085	46.613	44.895	7.570
20	16	40	0.5	1	12.5	200	4.005×10^{-4}	16.954	0.0086	56.625	55.225	8.832
20	16	40	2.5	1	12.5	200	3.222×10^{-4}	20.218	0.0088	39.956	37.918	9.189
20	16	40	1.5	3	12.5	200	5.186×10^{-4}	29.139	0.0078	75.951	73.862	7.344
20	16	40	1.5	6	12.5	200	5.265×10^{-4}	25.000	0.0025	116.834	115.548	4.779
20	16	40	1.5	1	4	200	1.825×10^{-4}	49.998	0.0048	135.542	133.776	7.240
20	16	40	1.5	1	8	200	2.228×10^{-4}	47.209	0.0081	95.213	92.249	8.170
20	16	40	1.5	1	12.5	50	2.583×10^{-4}	27.910	0.0219	2.095	1.937	2.656
20	16	40	1.5	1	12.5	100	2.801×10^{-4}	39.799	0.0123	9.106	8.898	4.885
20	16	40	1.5	1	12.5	150	3.834×10^{-4}	35.264	0.0108	28.244	27.376	7.097
20	16	40	1.5	1	12.5	500	9.573×10^{-5}	17.091	0.0064	229.359	227.658	13.649

capacity of CR decreased from 8.924 to 4.780 mg g^{-1} with an increase in flow rate of dye solution from 1 to 6 mL min^{-1}. This may be due to insufficient contact time for the dye molecules with the live biomass and wheat bran inside the reactor and diffusional limitation of the solute into the pores of the dual adsorbent [7]. The predicted and experimental values of effluent dye concentrations at equilibrium (S_e) are compared and these values are reported in Table 2. It shows that the predicted S_e values obtained from the developed model are in good agreement with experimental S_e values. The experimental and predicted values of effluent concentration (S) at various inlet dyestuff concentrations of 50, 100, 200, and 500 mg L^{-1} are shown in Figs. 3–6 and Tables S1–S4, respectively. As seen in Figs. 3–6, the predicted values of S found from the model fitted well to the experimental values. The values of SSE are in the range between 0.0022 and 0.0155 at various dyestuff concentrations ranging from 50 to 500 mg L^{-1} (Tables S1–S4). It signifies that the combined Monod and pseudo-second-order kinetic model is valid for CR dye decolorization. Monod model assumes that a single substrate is growth-rate limiting [47] and pseudo-second-order kinetic model assumes that chemisorption mechanism is the rate-controlling step in the biosorption process [48]. The regeneration of live biomass in the desorption studies is very limited since most toxicants are intracellularly accumulated, hence, the biomass cannot be utilized for the next cycles [49].

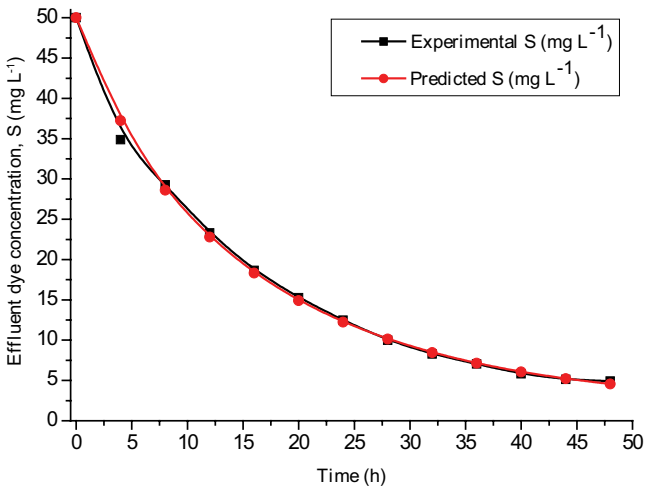

Fig. 3. Substrate concentration profile for real-time vs. simulated values at CR dye concentration of 50 mg L^{-1} in the RBC reactor. (Initial pH: 6; wheat bran dosage: 12.5 g L^{-1}; flow rate of dye solution: 1 mL min^{-1}; air flow rate: 1.5 L min^{-1}; number of discs: 20; disc rotation speed: 16 rpm; disc submergence in liquid medium: 40%; temperature: 303 K; effluent treatment time: 48 h; volume of liquid in the reactor: 12 L).

4. Conclusion

The surface immobilized live fungal biomass of *N. crassa* with wheat bran may be used as an effective material for the decolorization CR from synthetic dye wastewater in a RBC reactor. RTD studies showed that the value of dispersion number at various flow rates of water such as 1, 3, and 6.5 mL min^{-1} are 4.36, 7.89, and 13.65, respectively (dispersion number increased with increase in flow rate of water) which illustrates that the RBC reactor can be modeled as a

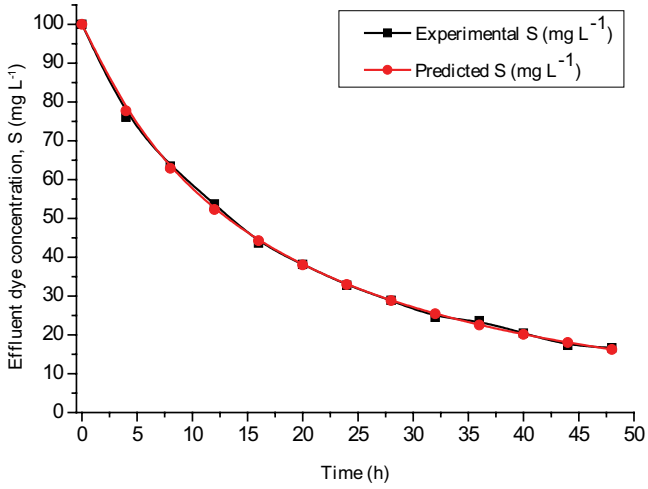

Fig. 4. Substrate concentration profile for real-time vs. simulated values at CR dye concentration of 100 mg L^{-1} in the RBC reactor. (Initial pH: 6; wheat bran dosage: 12.5 g L^{-1}; flow rate of dye solution: 1 mL min^{-1}; air flow rate: 1.5 L min^{-1}; number of discs: 20; disc rotation speed: 16 rpm; disc submergence in liquid medium: 40%; temperature: 303 K; effluent treatment time: 48 h; volume of liquid in the reactor: 12 L).

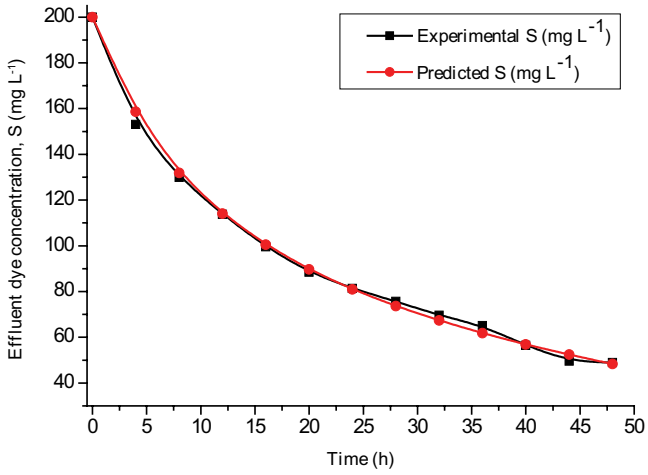

Fig. 5. Substrate concentration profile for real-time vs. simulated values at CR dye concentration of 200 mg L^{-1} in the RBC reactor. (Initial pH: 6; wheat bran dosage: 12.5 g L^{-1}; flow rate of dye solution: 1 mL min^{-1}; air flow rate: 1.5 L min^{-1}; number of discs: 20; disc rotation speed: 16 rpm; disc submergence in liquid medium: 40%; temperature: 303 K; effluent treatment time: 48 h; volume of liquid in the reactor: 12 L).

mixed flow reactor. It shows that, as the fluid flows through the reactor, there is a significant degree of dispersion taking place and the concentration of the tracer spreads in the effluent uniformly throughout the reactor. The predicted values of effluent dye concentrations found from the developed model (combined Monod and pseudo-second-order kinetic model) fitted well to the experimental data. It suggests that the proposed model is valid for CR dye decolorization and the parameters estimated from the model can be used to design a large-scale reactor. The experimental results

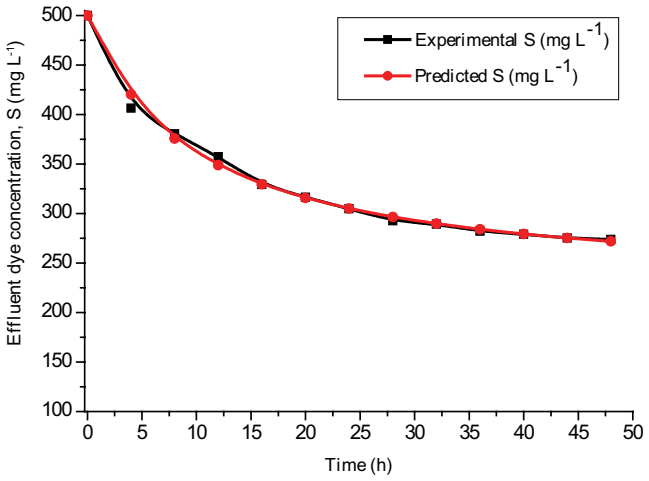

Fig. 6. Substrate concentration profile for real-time vs. simulated values at CR dye concentration of 500 mg L^{-1} in the RBC reactor. (Initial pH: 6; wheat bran dosage: 12.5 g L^{-1}; flow rate of dye solution: 1 mL min^{-1}; air flow rate: 1.5 L min^{-1}; number of discs: 20; disc rotation speed: 16 rpm; disc submergence in liquid medium: 40%; temperature: 303 K; effluent treatment time: 48 h; volume of liquid in the reactor: 12 L).

showed that the PU surface immobilized live fungal biomass of *N. crassa* with wheat bran adsorbent/substrate can be used effectively to remove other anionic dyes from industrial effluents. The accuracy of the predicted data suggests that the developed model may be valid for dye wastewater treatment.

Symbols and abbreviations

A	—	Mass of CR dye solution, g
A_w	—	Total surface area of the bio-disc, m^2
CR	—	Congo red dye
CSTR	—	Continuous stirred tank reactor
D_{SL}	—	% disc submergence in liquid medium
D_Z	—	Axial dispersion coefficient, m^2 s^{-1}
D_Z/UL	—	Dispersion number
dS/dt	—	Change in substrate concentration with time, mg L^{-1} h^{-1}
$E(t)$	—	Residence-time distribution function, h^{-1}
$E(\theta)$	—	Normalized RTD function
F	—	Flow rate of dye solution, mL min^{-1}
K_s	—	Monod kinetic constant, mg L^{-1}
K_2	—	Equilibrium rate constant of pseudo-second-order biosorption, g mg^{-1} h^{-1}
L	—	L is the length of the reactor, m
M	—	Mass of component "A" in the reactor, g
M_i	—	Mass flow rate of "A" entering to the reactor, g h^{-1}
M_0	—	Mass flow rate of "A" leaving from the reactor, g h^{-1}
MEB	—	Malt extract broth
M_{LB-WB}	—	Mass of attached active live fungal biomass and wheat bran (g) existing in the reactor before treatment of dye wastewater at time $t = 0$
M_{WB}	—	Concentration of wheat bran added in the reactor, g L^{-1}

N — Disc rotation speed, rpm
N_D — Number of discs
ODE — Ordinary differential equation
PU — Polyurethane foam
Q_{air} — Air flow rate, L min^{-1}
q_e — Amount of dye adsorbed on the surface of live biomass and wheat bran at equilibrium, mg g^{-1}
q_t — Amount of dye adsorbed on the adsorbent surface of live biomass and wheat bran at any time t, mg g^{-1}
R_{Ad} — Rate of mass biosorption of "A" by wheat bran and live biomass in the reactor, g h^{-1}
R_C — Rate of mass consumption of "A" by reaction, g h^{-1}
R_{Ca} — Rate of substrate consumption by attached growth, g h^{-1}
R_{Cs} — Rate of substrate consumption by suspended growth, g h^{-1}
R_G — Rate of mass generation of "A" by reaction, g h^{-1}
RBC — Rotating biological contactor
RTD — Residence time distribution
S — Effluent substrate (dye) concentration at time t, mg L^{-1}
S_0 — Influent substrate (dye) concentration, mg L^{-1}
S_e — Effluent substrate (dye) concentration at equilibrium, mg L^{-1}
S_{expt} — Experimental value of effluent substrate concentration at time t, mg L^{-1}
S_{pred} — Predicted value of effluent substrate concentration at time t, mg L^{-1}
SSE — Sum of square error
t — Effluent treatment time at time t, h
t_0 — Effluent treatment time at time t = 0, h
t_m — Mean residence time, h
U — Superficial velocity, m s^{-1}
V — Liquid volume in the reactor, L
X_a — Mass of attached active biomass per unit area of bio-disc, mg m^{-2}
X_d — Amount of attached biomass per unit area of bio-disc in dye medium, mg m^{-2}
X_f — Concentration of attached active biomass in dye medium, mg L^{-1}
X_n — Amount of attached biomass per unit area of bio-disc in MEB medium, mg m^{-2}
X_0 — Concentration of attached active biomass in MEB medium, mg L^{-1}
X_s — Concentration of suspended biomass, mg L^{-1}
Y_a — Apparent yield coefficient of the attached biomass
Y_s — Apparent yield coefficient of the suspended biomass

Greek letters

θ — Dimensionless parameter
σ^2 — Variance, h^2
τ — Space time, h
μ_a — Specific growth rate of the attached biomass, h^{-1}
μ_s — Specific growth rate of the suspended biomass, h^{-1}
μ_{max} — Maximum growth rate of attached active biomass, h^{-1}

References

[1] U. Habiba, T.C. Joo, S.K.A. Shezan, R. Das, B.C. Ang, A.M. Afifi, Synthesis and characterization of chitosan/TiO_2 nanocomposite for the adsorption of Congo red, Desal. Water Treat., 164 (2019) 361–367.
[2] A. Sharma, Z.M. Siddiqui, S. Dhar, P. Mehta, D. Pathania, Adsorptive removal of congo red dye (CR) from aqueous solution by *Cornulaca monacantha* stem and biomass-based activated carbon: isotherm, kinetics and thermodynamics, Sep. Sci. Technol., 54 (2019) 916–929.
[3] A. Azari, R. Rezaei, H. Sanaeepur, Synthesis and characterization of TiO_2 nanoparticles loaded activated carbon for Congo Red removal from wastewater: kinetic and equilibrium studies, Desal. Water Treat., 124 (2018) 308–318.
[4] P. Vairavel, V. Ramachandra Murty, Optimization, kinetics, equilibrium isotherms and thermodynamics studies for Congo red dye adsorption using calcium alginate beads immobilized with dual adsorbent (*Neurospora crassa* dead fungal biomass and wheat bran), Desal. Water Treat., 97 (2017) 338–362.
[5] Z.A. Medvedev, H.M. Crowne, M.N. Medvedeva, Age related variations of hepatocarcinogenic effect of azo dye (3′-MDAB) as linked to the level of hepatocyte polyploidization, Mech. Ageing Dev., 46 (1988) 159–174.
[6] S. Vahidhabanu, I. Swathika, A.I. Adeogun, R. Roshni, B.R. Babu, Biomass-derived magnetically tuned carbon modified Sepiolite for effective removal of Congo red from aqueous solution, Desal. Water Treat., 184 (2020) 326–339.
[7] P. Vairavel, V. Ramachandra Murty, Continuous fixed-bed adsorption of Congo red dye by dual adsorbent (*Neurospora crassa* dead fungal biomass and wheat bran): experimental and theoretical breakthrough curves, immobilization and reusability studies, Desal. Water Treat., 98 (2017) 276–293.
[8] A.A. Mizhir, A.A. Abdulwahid, H.S. Al-Lami, Adsorption of carcinogenic dye Congo red onto prepared graphene oxide-based composites, Desal. Water Treat., 202 (2020) 381–395.
[9] L.B.L. Lim, N. Priyantha, S.A.A. Latip, Y.C. Lu, A.H. Mahadi, Converting *Hylocereus undatus* (white dragon fruit) peel waste into a useful potential adsorbent for the removal of toxic Congo red dye, Desal. Water Treat., 185 (2020) 307–317.
[10] J. Mohanta, D. Banashree, D. Soumen, Highly porous iron-zirconium binary oxide for efficient removal of Congo red from water, Desal. Water Treat., 189 (2020) 227–242.
[11] C. Srilakshmi, R. Saraf, Ag-doped hydroxyapatite as efficient adsorbent for removal of Congo red dye from aqueous solutions: synthesis, kinetic and equilibrium adsorption isotherm analysis, Microporous Mesoporous Mater., 219 (2016) 134–144.
[12] K. Wen, Y. Li, Z. Shuxing, Z. Xiaoting, R. Han, Adsorption of Congo red from solution by iron doped PVA-chitosan composite film, Desal. Water Treat., 187 (2020) 378–389.
[13] P. Vairavel, V. Ramachandra Murty, S. Nethaji, Removal of Congo red dye from aqueous solutions by adsorption onto a dual adsorbent (*Neurospora crassa* dead biomass and wheat bran): optimization, isotherm, and kinetics studies, Desal. Water Treat., 68 (2017) 274–292.
[14] X. Mi, Z. Shang, C. Du, G. Li, T. Su, X. Chang, R. Li, Z. Zheng, J. Tie, Adsorption of an anionic azo dye using *Moringa oleifera* seed protein-montmorillonite composite, J. Chem., 2019 (2019) 1–8.
[15] M. Abbas, T. Aksil, M. Trari, Removal of toxic methyl green (MG) in aqueous solutions by apricot stone activated carbon – equilibrium and isotherms modelling, Desal. Water Treat., 125 (2018) 93–101.
[16] K. Pakshirajan, S. Singh, Decolorization of synthetic wastewater containing azo dyes in a batch-operated rotating biological contactor reactor with the immobilized fungus *Phanerochaete chrysosporium*, Ind. Eng. Chem. Res., 49 (2010) 7484–7487.
[17] K. Pakshirajan, S. Kheria, Continuous treatment of coloured industry wastewater using immobilized *Phanerochaete chrysosporium* in a rotating biological contactor reactor, J. Environ. Manage., 101 (2012) 118–123.

[18] S.K. Sen, S. Raut, P. Bandyopadhyay, S. Raut, Fungal decolouration and degradation of azo dyes: a review, Fungal Biol. Rev., 30 (2016) 112–133.
[19] K.A. Adegoke, O.S. Bello, Dye sequestration using agricultural wastes as adsorbents, Water Resour. Ind., 12 (2015) 8–24.
[20] P. Vairavel, V. Ramachandra Murty, Decolorization of Congo red dye in a continuously operated rotating biological contactor reactor, Desal. Water Treat., 196 (2020) 299–314.
[21] J.T. Adeosun, A. Lawal, Numerical and experimental studies of mixing characteristics in a T-junction microchannel using residence-time distribution, Chem. Eng. Sci., 64 (2009) 2422–2432.
[22] P. Vairavel, V. Ramachandra Murty, Optimization of batch process parameters for Congo red color removal by *Neurospora crassa* live fungal biomass with wheat bran dual adsorbent using response surface methodology, Desal. Water Treat., 103 (2018) 84–101.
[23] T. Akar, T.A. Demir, I. Kiran, A. Ozcan, A.S. Ozcan, S. Tunali, Biosorption potential of *Neurospora crassa* cells for decolorization of Acid Red 57 dye, J. Chem. Technol. Biotechnol., 81 (2006) 1100–1106.
[24] I. Kiran, T. Akar, S. Tunali, Biosorption of Pb(II) and Cu(II) from aqueous solutions by pretreated biomass of *Neurospora crassa*, Process Biochem., 40 (2005) 3550–3558.
[25] M.S. Manocha, J.R. Colvin, Structure and composition of cell wall of *Neurospora crassa*, J. Bacteriol., 94 (1967) 202–212.
[26] X. Sun, Z. Liu, Y. Qu, X. Li, The effects of wheat bran composition on the production of biomass-hydrolyzing enzymes by *Penicillium decumbens*, Appl. Biochem. Biotechnol., 146 (2008) 119–128.
[27] G. Banerjee, Hydraulics of bench-scale rotating biological contactor, Water Res., 31 (1997) 2500–2510.
[28] P. Teixeira, M. Alves, R. Oliveira, Hydraulic characteristics of an anoxic rotating biological contactor: influence of biofilm, Environ. Technol., 22 (2001) 1169–1175.
[29] S. Leveneur, J. Warna, K. Eranen, T. Salmi, Green process technology for peroxycarboxylic acids: estimation of kinetic and dispersion parameters aided by RTD measurements: green synthesis of peroxycarboxylic acids, Chem. Eng. Sci., 66 (2011) 1038–1050.
[30] T.J. Rector, J.L. Garland, S.O. Starr, Dispersion characteristics of a rotating hollow fiber membrane bioreactor: Effects of module packing density and rotational frequency, J. Membr. Sci., 278 (2006) 144–150.
[31] H.S. Fogler, Elements of Chemical Reaction Engineering, 5th ed, Pearson Prentice Hall Limited, USA, 2016.
[32] S.A.M. Moreno, R.P. Cadena, A.J. Gonzalez, A.T. Jurado, C.A.L. Constantino, Modeling wastewater biodecolorization with reactive blue 4 in fixed bed bioreactor by *Trametes subectypus*: biokinetic, biosorption and transport, Bioresour. Technol., 123 (2012) 452–462.
[33] M.R.C. Diaz, E.P. Rivero, F.J.A. Ruiz, A.T. Mendoza, I. Gonzalez, Design of a new FM01-LC reactor in parallel plate configuration using numerical simulation and experimental validation with residence time distribution (RTD), Chem. Eng. Process., 85 (2014) 145–154.
[34] J.H. Clark, E.M. Moseng, T. Asano, Performance of a rotating biological contactor under varying wastewater flow, J. Water Pollut. Control Fed., 50 (1978) 896–911.
[35] P.M. Doran, Bioprocess Engineering Principles, 2nd ed., Elsevier Science and Technology Publishing Company Limited, Academic Press, UK, 1995.
[36] L.D. Palma, C. Merli, M. Paris, E. Petrucci, A steady-state model for the evaluation of disk rotational speed influence on RBC kinetic: model presentation, Bioresour. Technol., 86 (2003) 193–200.
[37] Y.S. Ho, G. McKay, Pseudo-second order model for sorption processes, Process Biochem., 34 (1999) 451–465.
[38] C. Debamita, R. Nakul, J.P. Gautham, P. Vairavel, Process optimization, isotherm, kinetics, and thermodynamics studies for removal of Remazol Brilliant Blue – R dye from contaminated water using adsorption on guava leaf powder, Desal. Water Treat., 185 (2020) 318–343.
[39] J.M. Divya, K. Palak, P. Vairavel, Optimization, kinetics, equilibrium isotherms, and thermodynamics studies of Coomassie violet dye adsorption using *Azadirachta indica* (neem) leaf adsorbent, Desal. Water Treat., 190 (2020) 353–382.
[40] F. Kargi, S. Eker, Performance of rotating perforated tubes biofilm reactor in biological wastewater treatment, Enzyme Microb. Technol., 32 (2003) 464–471.
[41] J.A. Robinson, J.M. Tiedje, Nonlinear estimation of Monod growth kinetic parameters from a single substrate depletion curve, Appl. Environ. Microbiol., 45 (1983) 1453–1458.
[42] D.B. Spengel, D.A. Dzombak, Biokinetic modeling and scale-up considerations for rotating biological contactors, Water Environ. Res., 64 (1992) 223–235.
[43] S. Cetintas, S. Elevli, D. Bingol, Comparison of regression and design models for biosorption process, Desal. Water Treat., 145 (2019) 107–119.
[44] M. Rodgers, X.M. Zhan, B. Dolan, Mixing characteristics and whey wastewater treatment of a novel moving anaerobic biofilm reactor, J. Environ. Sci. Health., Part A, 39 (2004) 2183–2193.
[45] O. Levenspiel, Chemical Reaction Engineering, 3rd ed, John Wiley and Sons, New Jersey, USA, 1999.
[46] C. Forster, Anaerobic digestion and industrial wastewater treatment, Chem. Ind., 6 (1994) 404–406.
[47] M.L. Shuler, F. Kargi, Bioprocess Engineering Basic Concepts, 2nd ed, Prentice Hall Publishing Company Limited, New Jersey, USA, 2003.
[48] C. Meghana, B. Juhi, N. Rampal, P. Vairavel, Isotherm, kinetics, process optimization and thermodynamics studies for removal of Congo red dye from aqueous solutions using *Nelumbo nucifera* (lotus) leaf adsorbent, Desal. Water Treat., 207 (2020) 373–397.
[49] K. Vijayaraghavan, Y. Yun, Bacterial biosorbents and biosorption: research review paper, Biotechnol. Adv., 26 (2008) 266–291.

Supplementary information

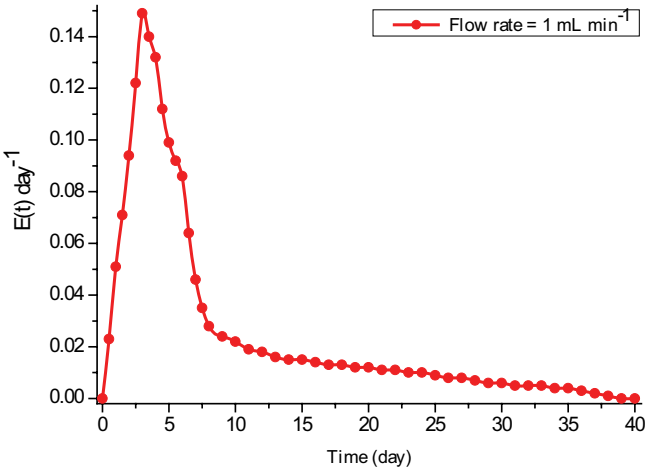

Fig. S1. E-curve profile of experimental data obtained from RTD studies in a RBC reactor at a flow rate of water 1 mL min^{-1}. (Volume of liquid in the reactor: 12 L; air flow rate: 1.5 L min^{-1}; number of discs: 20; disc rotation speed: 16 rpm; disc submergence in liquid medium: 40%; temperature: 303 K).

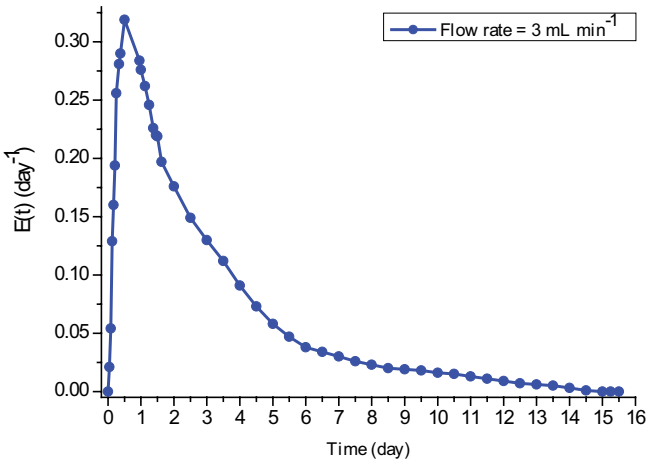

Fig. S2. E-curve profile of experimental data obtained from RTD studies in a RBC reactor at a flow rate of water 3 mL min^{-1}. (Volume of liquid in the reactor: 12 L; air flow rate: 1.5 L min^{-1}; number of discs: 20; disc rotation speed: 16 rpm; disc submergence in liquid medium: 40%; temperature: 303 K).

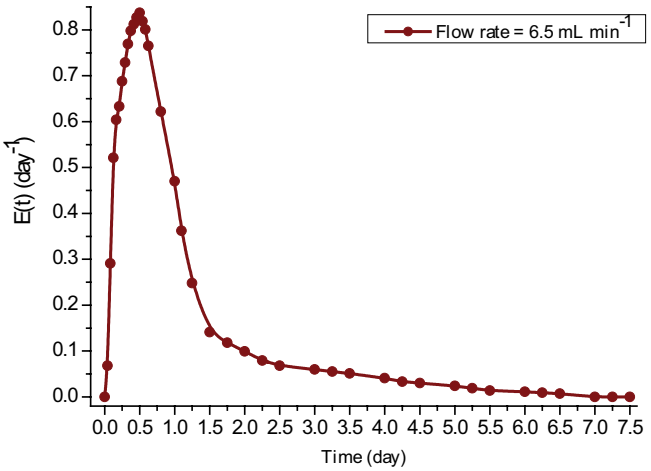

Fig. S3. E-curve profile of experimental data obtained from RTD studies in a RBC reactor at a flow rate of water 6.5 mL min^{-1}. (Volume of liquid in the reactor: 12 L; air flow rate: 1.5 L min^{-1}; number of discs: 20; disc rotation speed: 16 rpm; disc submergence in liquid medium: 40%; temperature: 303 K).

Table S1
Comparison of experimental and predicted values of effluent dye concentration (S) on CR decolorization in the RBC reactor at inlet dye concentration of 50 mg L^{-1}

Time (h)	S_{expt} (mg L^{-1})	S_{pred} (mg L^{-1})	% CR color removal
4	34.88	37.24	30.24
8	29.27	28.61	41.46
12	23.31	22.78	53.37
16	18.66	18.32	62.68
20	15.25	14.90	69.5
24	12.47	12.23	75.07
28	9.98	10.13	80.03
32	8.29	8.46	85.42
36	7.05	7.13	87.9
40	5.82	6.07	88.37
44	5.13	5.23	89.75
48	4.92	4.55	90.15
Sum of square error = 0.015592			

Table S2
Comparison of experimental and predicted values of effluent dye concentration (S) on CR decolorization in the RBC reactor at inlet dye concentration of 100 mg L^{-1}

Time (h)	S_{expt} (mg L^{-1})	S_{pred} (mg L^{-1})	% CR color removal
4	76.04	77.69	23.96
8	63.45	62.87	36.55
12	53.72	52.38	46.28
16	43.65	44.25	56.35
20	38.16	37.98	61.84
24	32.76	32.97	67.24
28	28.91	28.85	71.09
32	24.53	25.43	75.47
36	23.64	22.56	76.36
40	20.42	20.12	79.58
44	17.26	18.04	82.74
48	16.64	16.26	83.36
Sum of square error = 0.00779			

Table S3
Comparison of experimental and predicted values of effluent dye concentration (S) on CR decolorization in the RBC reactor at inlet dye concentration of 200 mg L^{-1}

Time (h)	S_{expt} (mg L^{-1})	S_{pred} (mg L^{-1})	% CR color removal
4	153.08	158.60	23.46
8	129.85	131.86	35.07
12	113.76	114.09	43.12
16	99.55	100.42	50.22
20	88.43	89.69	55.78
24	81.29	80.96	59.35
28	75.64	73.63	62.18
32	69.56	67.37	65.22
36	65.04	61.81	67.48
40	56.48	56.89	71.76
44	49.52	52.44	75.24
48	48.98	48.36	75.52
Sum of square error = 0.00972			

Table S4
Comparison of experimental and predicted values of effluent dye concentration (S) on CR decolorization in the RBC reactor at inlet dye concentration of 500 mg L^{-1}

Time (h)	S_{expt} (mg L^{-1})	S_{pred} (mg L^{-1})	% CR color removal
4	406.39	420.31	18.72
8	380.56	375.64	23.89
12	357.31	348.75	28.54
16	329.20	329.62	34.16
20	316.35	315.63	36.73
24	304.82	304.94	39.04
28	292.70	296.5	41.46
32	289.24	289.68	42.18
36	282.10	284.04	43.58
40	279.00	279.31	44.20
44	275.20	275.27	44.96
48	273.82	271.79	45.24
Sum of square error = 0.002197			